chemistry

MDPI

Supporting Information for:

Enhancing of CO uptake in Metal-Organic Frameworks by linker functionalization. A Multi-scale theoretical study

Charalampos G. Livas [1], Emmanuel Tylianakis [1,2] & George E. Froudakis [1]

[1] Department of Chemistry, Voutes Campus, University of Crete, GR-71003 Heraklion Crete, Greece;

[2] Department of Materials Science and Technology, Voutes Campus, University of Crete, GR-71003 Heraklion Crete, Greece;

Ab-initio results.

In order to calculate the global minimum energy and identify the energetically most favorable configuration of the two monomers, various initial configurations for the dimer C_6H_5–X···CO were considered and optimized. Figure S1 shows the systems studied and their corresponding binding energies calculated at the MP2/6311++G** level of theory. The binding energies were corrected for the Basis Set Superposition Error (BSSE) with the Counterpoise (CP) method as proposed by Boys and Bernardi [23], since BSSE correction is important for nonbonding interactions. The equation used to calculate the final binding energy of a dimer is:

$$BE = E_{dimer} - E_{linker}^{ghost} - E_{CO}^{ghost} + \Delta E_{deform} \quad (1)$$

where E_{dimer} is the total energy of the dimer, E_{linker}^{ghost} is the energy of the Benzene linker calculated at the dimer geometry in the presence of the ghost basis of CO molecule, E_{CO}^{ghost} is the energy of CO calculated at the dimer geometry in the presence of the ghost basis of the benzene modified linker, and ΔE_{deform} is the deformation energy, defined as the difference between the isolated interacting molecules (CO and the Benzene modified linker) in the dimer geometry and their optimized structures. Figure S2 shows the global minimum configuration of all the complexes. All optimized structures are available upon requested

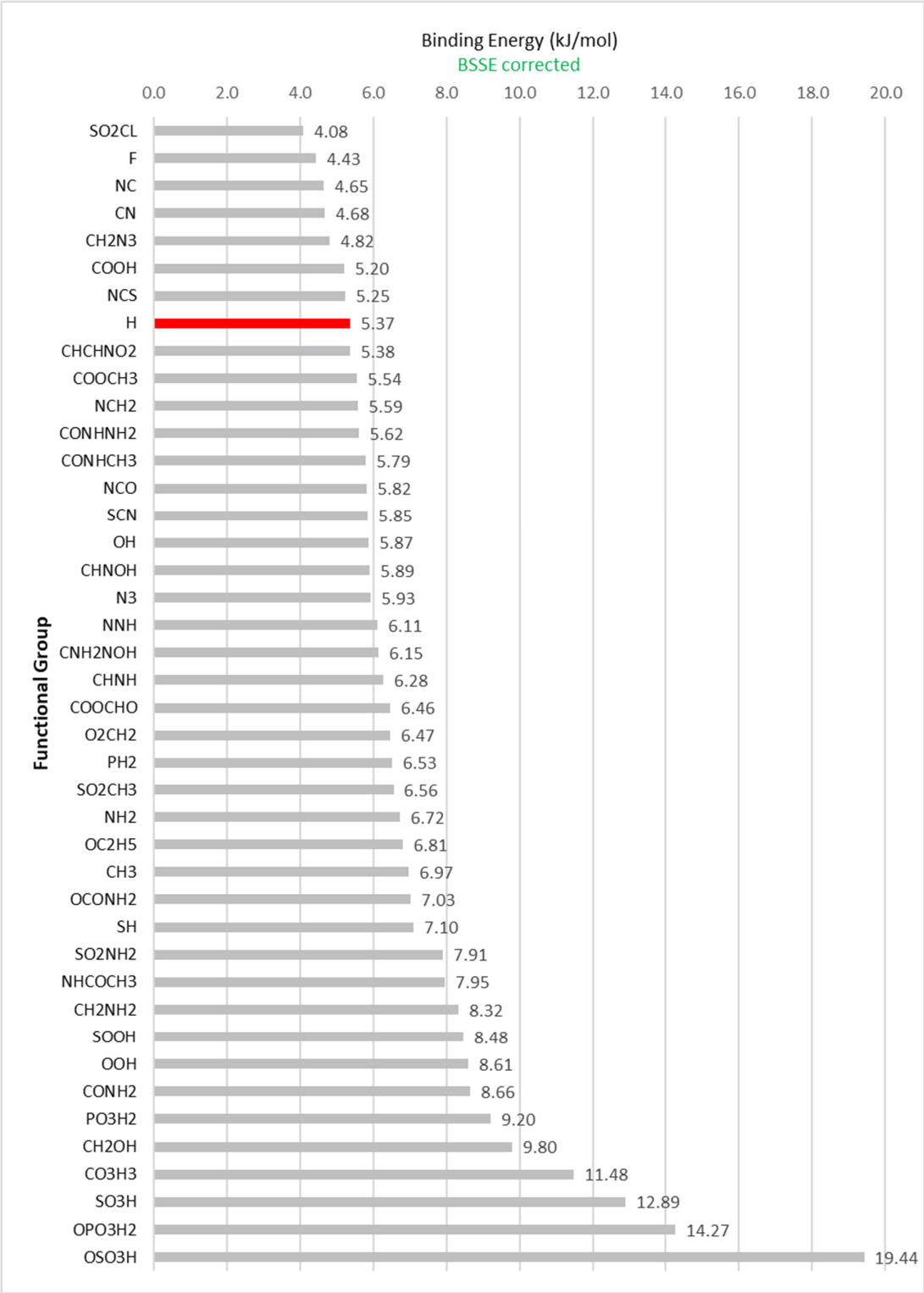

Figure S1: Sorted binding energies (kJ/mol) of the CO···C6H5-X systems under study, calculated at the MP2/6-311++G** level of theory. All interaction energy values have been corrected for the Basis Set Superposition Error (BSSE) by the full counterpoise method [23].

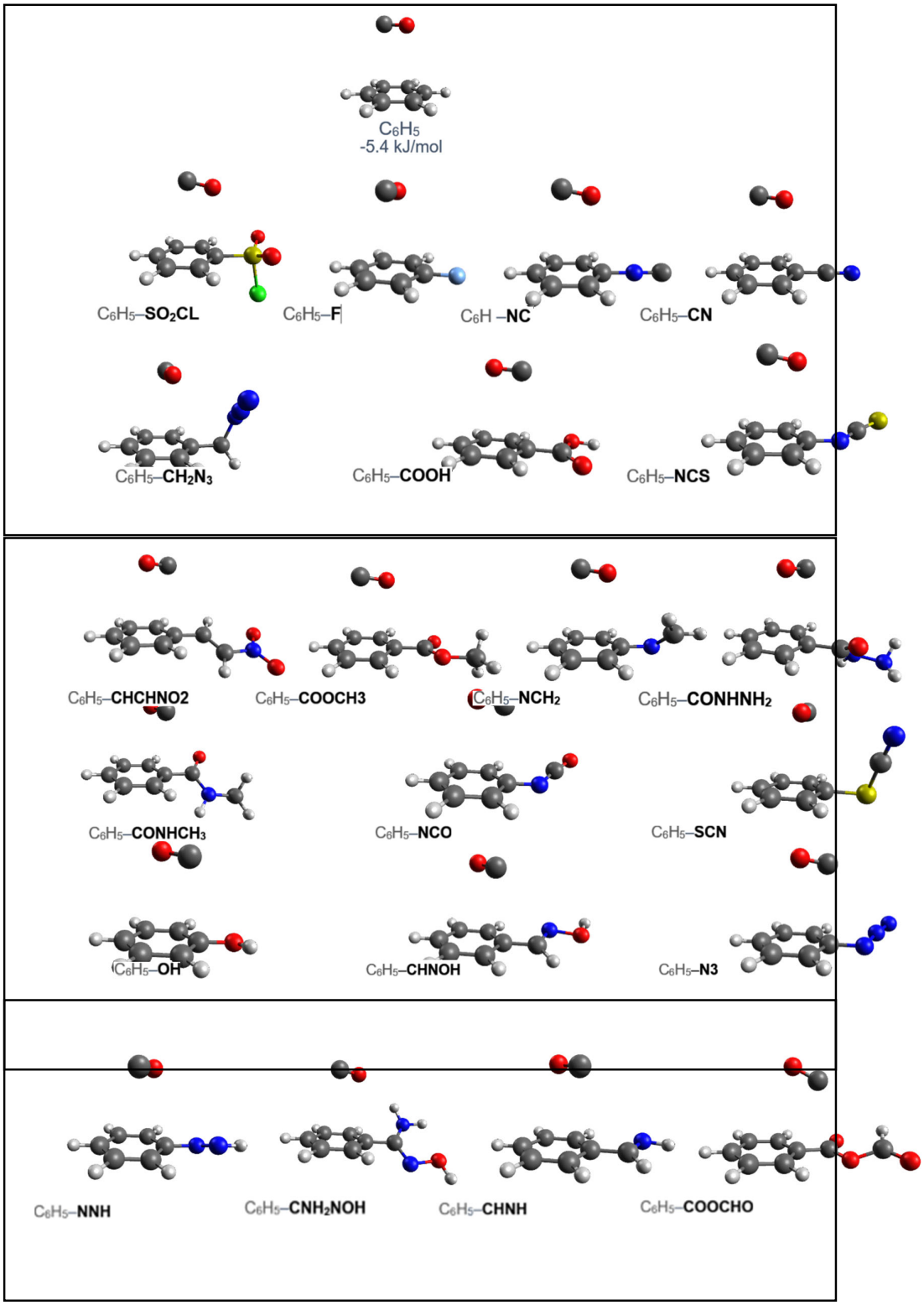
C6H5
-5.4 kJ/mol
C6H5–SO2CL
C6H5–F
C6H –NC
C6H5–CN
C6H5–CH2N3
C6H5–COOH
C6H5–NCS
C6H5–CHCHNO2
C6H5–COOCH3
C6H5–NCH2
C6H5–CONHNH2
C6H5–CONHCH3
C6H5–NCO
C6H5–SCN
C6H5–OH
C6H5–CHNOH
C6H5–N3
C6H5–NNH
C6H5–CNH2NOH
C6H5–CHNH
C6H5–COOCHO

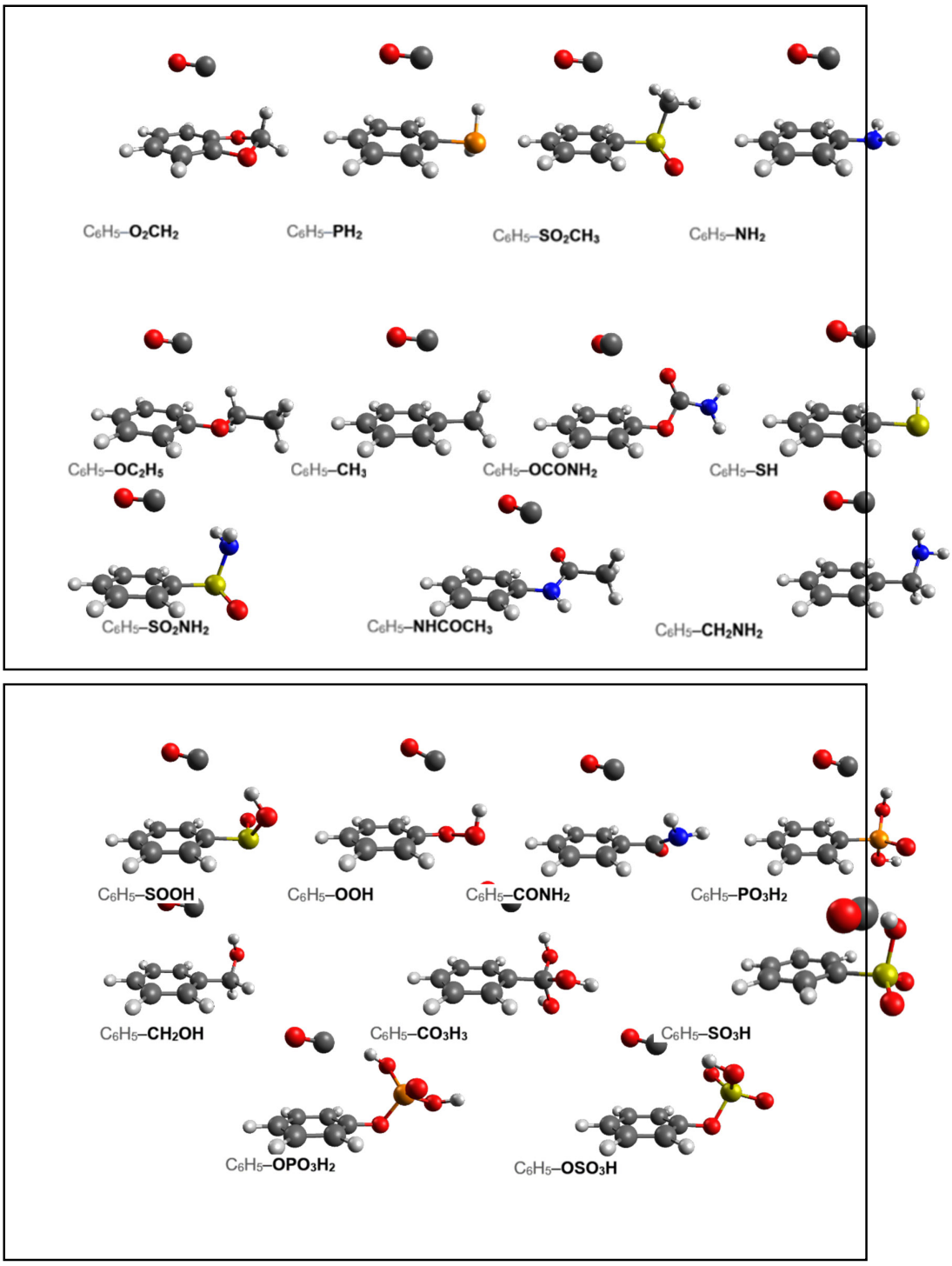

Figure S2: Global minima geometries of all the systems in this study.

For all the functionalized benzene molecules (C_6H_5-X) colored electrostatic potential maps were generated, by mapping the calculated electrostatic potentials onto the 0.001 au electron density isosurface, using gOpenMol [30, 31].

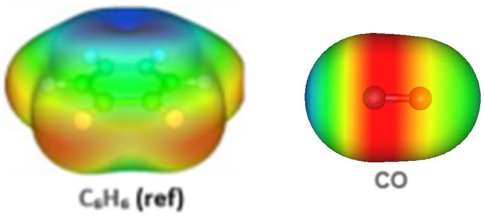
C6H6 (ref)
CO

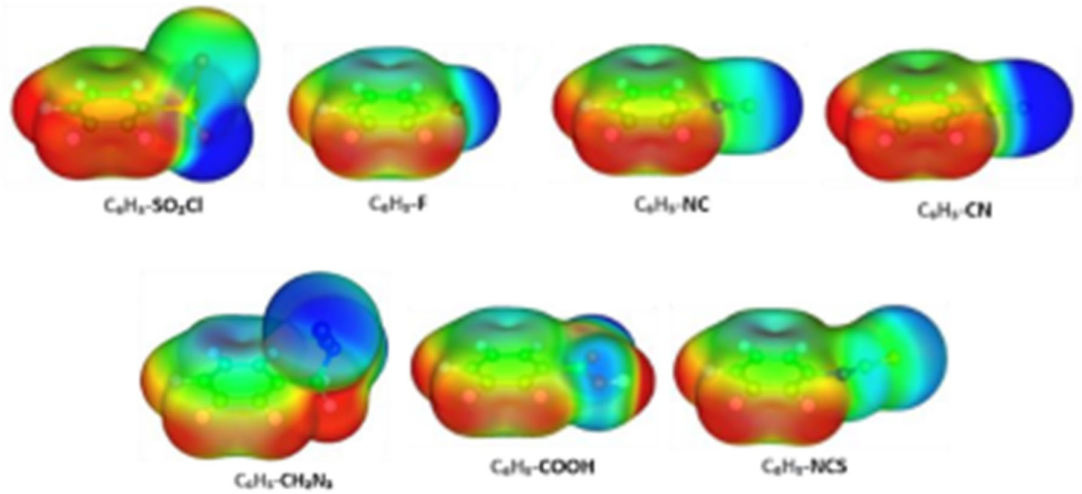
C6H5-SO2Cl
C6H5-F
C6H5-NC
C6H5-CN
C6H5-CH2N3
C6H5-COOH
C6H5-NCS

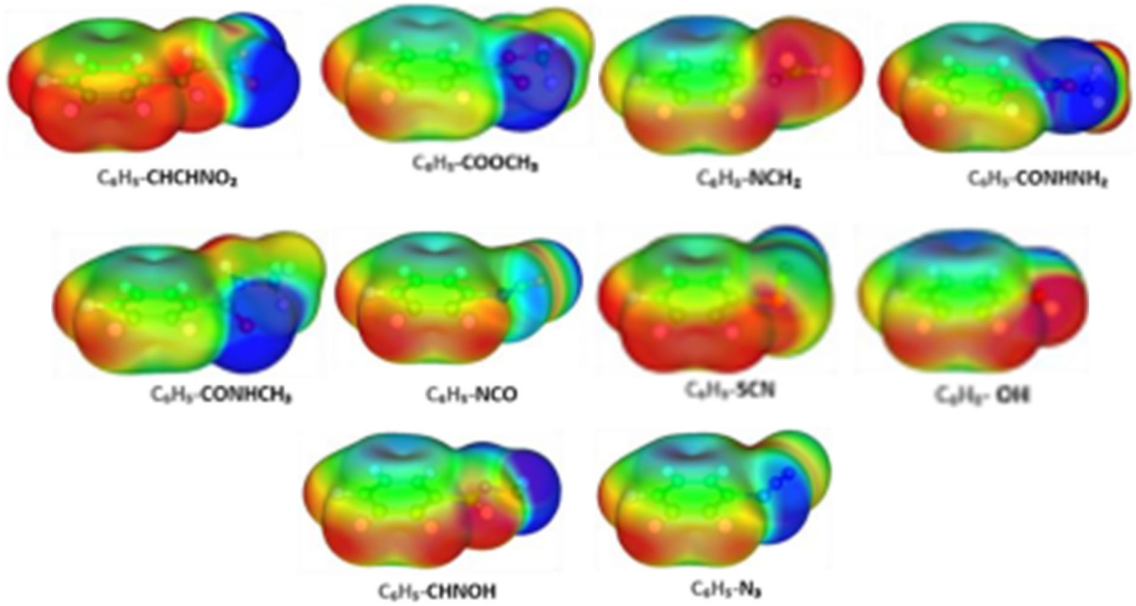
C6H5-CHCHNO2
C6H5-COOCH3
C6H5-NCH2
C6H5-CONHNH2
C6H5-CONHCH3
C6H5-NCO
C6H5-SCN
C6H5-OH
C6H5-CHNOH
C6H5-N3

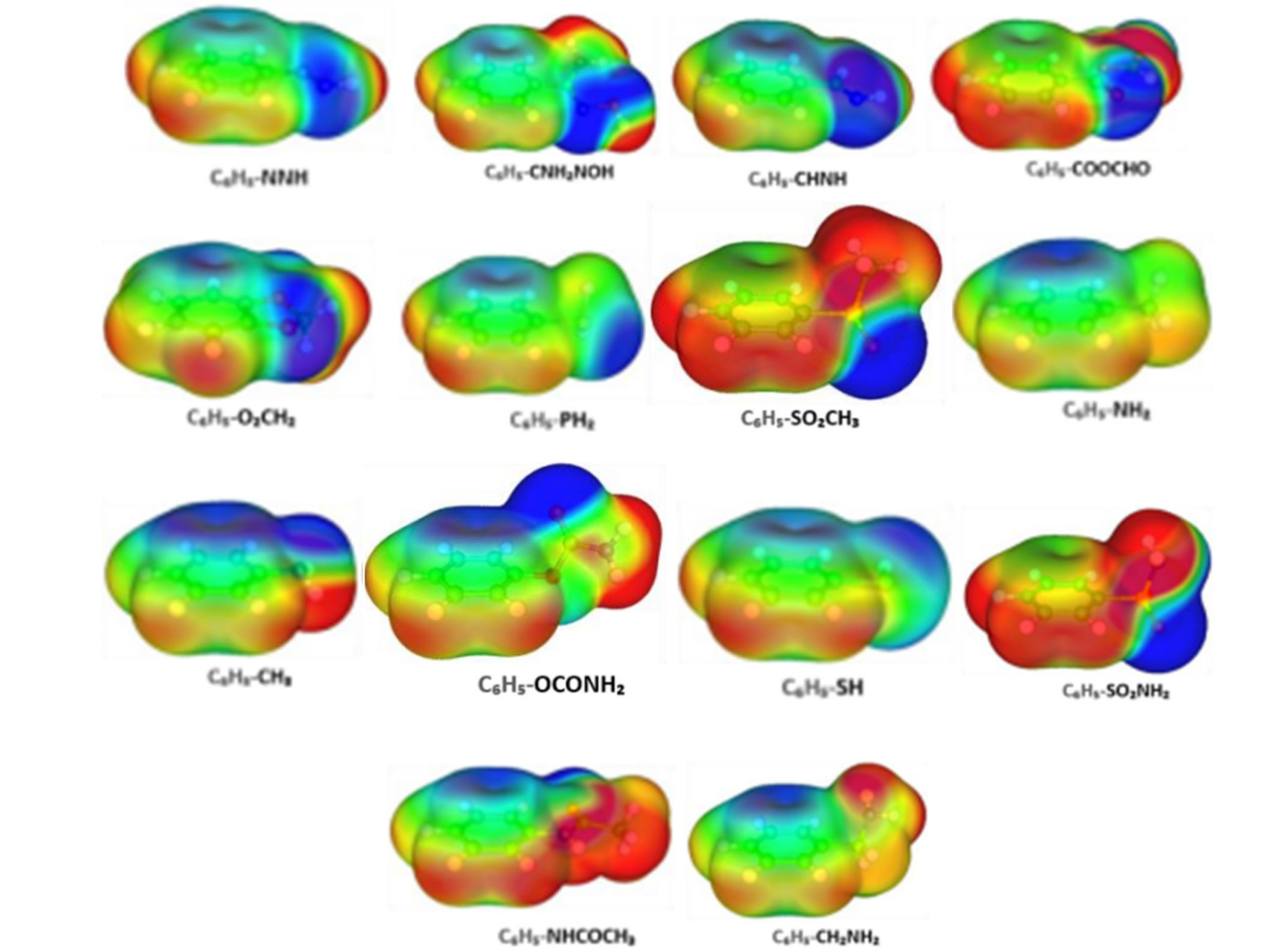
C6H5-NNH
C6H5-CNH2NOH
C6H5-CHNH
C6H5-COOCHO
C6H5-O2CH3
C6H5-PH2
C6H5-SO2CH3
C6H5-NH2
C6H5-CH3
C6H5-OCONH2
C6H5-SH
C6H5-SO2NH2
C6H5-NHCOCH3
C6H5-CH2NH2

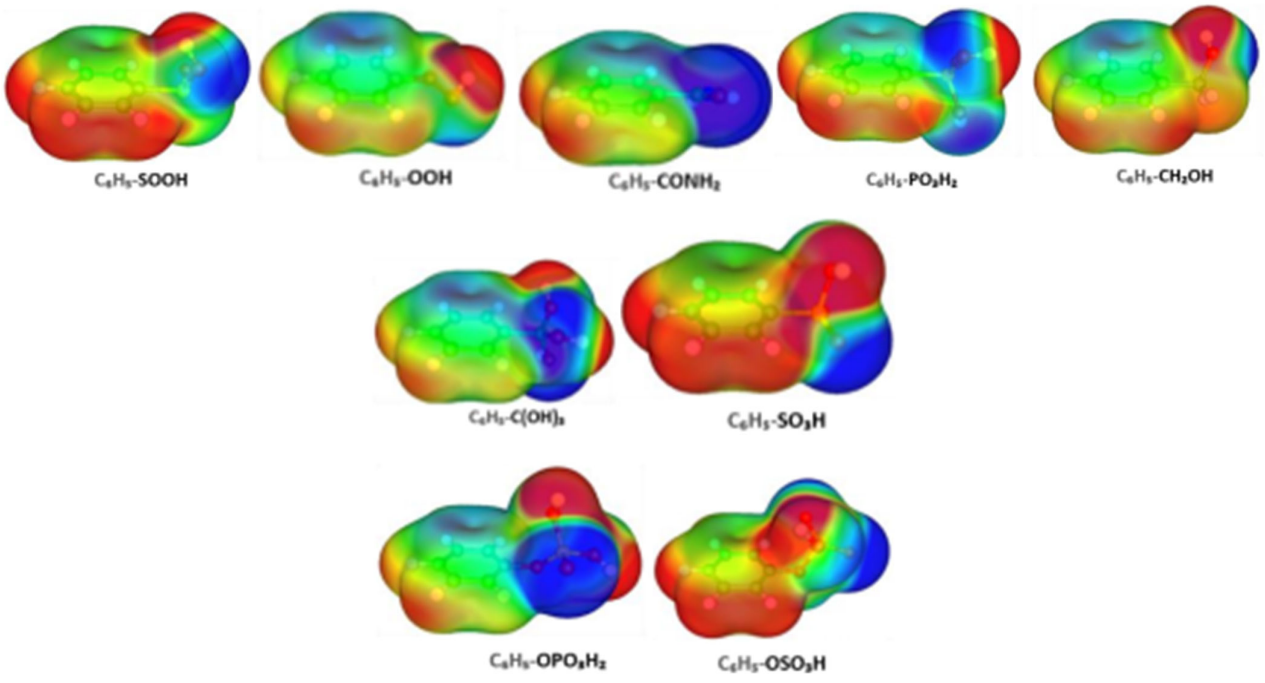
C6H5-SOOH
C6H5-OOH
C6H5-CONH2
C6H5-PO3H2
C6H5-CH2OH
C6H5-C(OH)3
C6H5-SO3H
C6H5-OPO3H2
C6H5-OSO3H

Figure S3: Electrostatic potential maps of the strongest interacting C6H5-X monomers. Calculated using the MP2 /6-311++G** method with ORCA 4.2 [21, 22] and visualized with gOpenMol. The varying intensities are ranging from -0.03 to +0.03 Hartree·e-1. Red: Electron-poor regions - high potential value, Blue: electron-rich regions - low potential.

It can be seen that the Carbon atom of the CO molecule is encompassed by a region of low electrostatic potential and the hydrogen atom of the top-performing FGs is enveloped by a region of high electrostatic potential. Taking into consideration the dimer complexes depicted in Figure S2, it can be concluded that there is an electrostatic interaction between the two atoms and that is the reason why the CO molecule orients itself that way.

Electron density redistribution plots were visualized at the MP2/6-311++G** level of theory, as the difference of the electron density of the dimer minus the sum of the isolated monomers within the conformation of the dimer. The density of each monomer at the complex geometry was calculated in the presence of ghost basis functions of the other monomer. Densities were plotted with a contour value of 0.001 au by using gOpenMol and are shown in Figure S4.

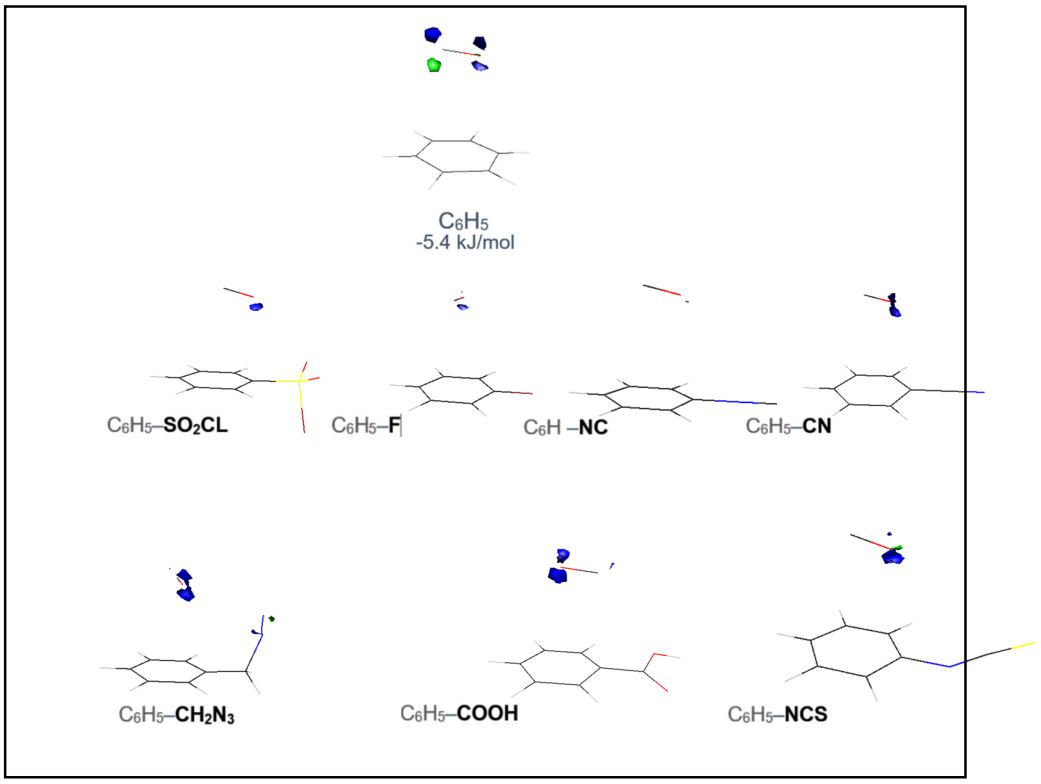

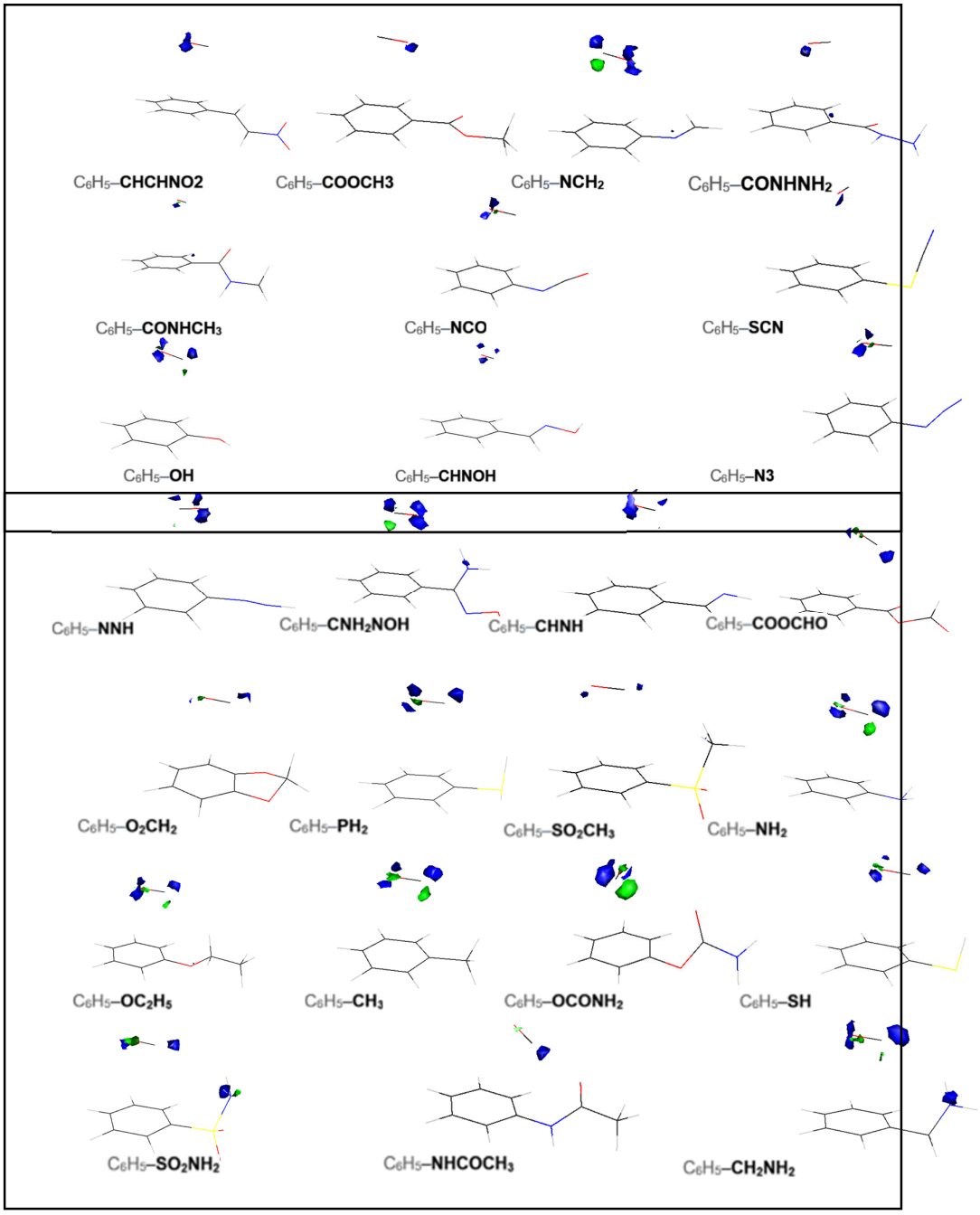
C6H5–CHCHNO2
C6H5–COOCH3
C6H5–NCH2
C6H5–CONHNH2
C6H5–CONHCH3
C6H5–NCO
C6H5–SCN
C6H5–OH
C6H5–CHNOH
C6H5–N3
C6H5–NNH
C6H5–CNH2NOH
C6H5–CHNH
C6H5–COOCHO
C6H5–O2CH2
C6H5–PH2
C6H5–SO2CH3
C6H5–NH2
C6H5–OC2H5
C6H5–CH3
C6H5–OCONH2
C6H5–SH
C6H5–SO2NH2
C6H5–NHCOCH3
C6H5–CH2NH2

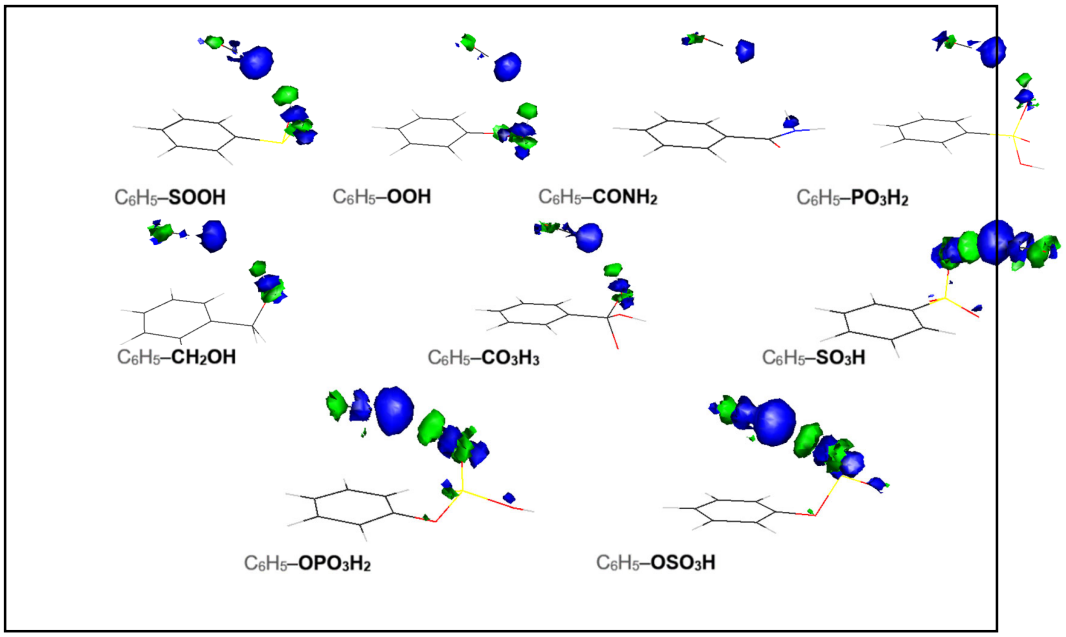

Figure S4: Electron-density redistribution plots of the optimized geometries of the CO···C6H5-X complexes. With blue and green the regions that gain and lose electron density upon the formation of the complex, respectively.

Ab-initio derived interatomic potential fitting

Rigid scans were performed at the MP2/6-311++G** level of theory to obtain the interaction energies between the Carbon Monoxide molecule and the C_6H_5-X monomer at selected distances around the global minimum. Each functional group contains many different atom-types with unique e,s parameters and must be fitted simultaneously. By fitting the specific curves for all different atoms using an in-home python algorithm, we get the parameter values for all atoms of the FG. All parameters were mixed using the Lorentz-Berthelot mixing rules [32, 33].

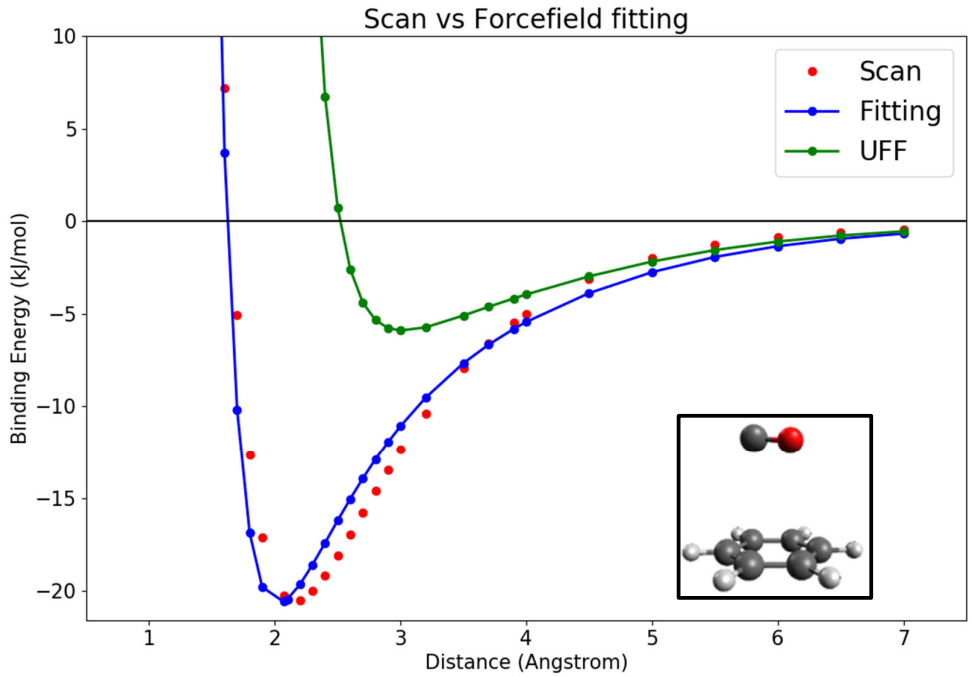

Figure S5: Fitting of the (ε, σ) parameters of the UFF potential [27] on the QM data obtained from the ab-initio scan of CO over benzene.

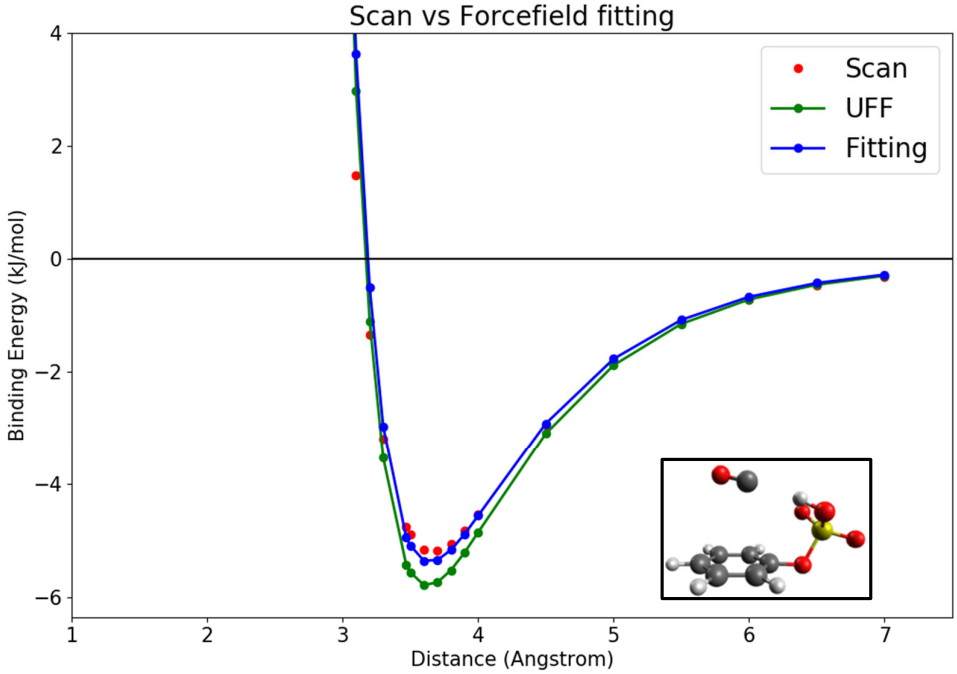

(a)

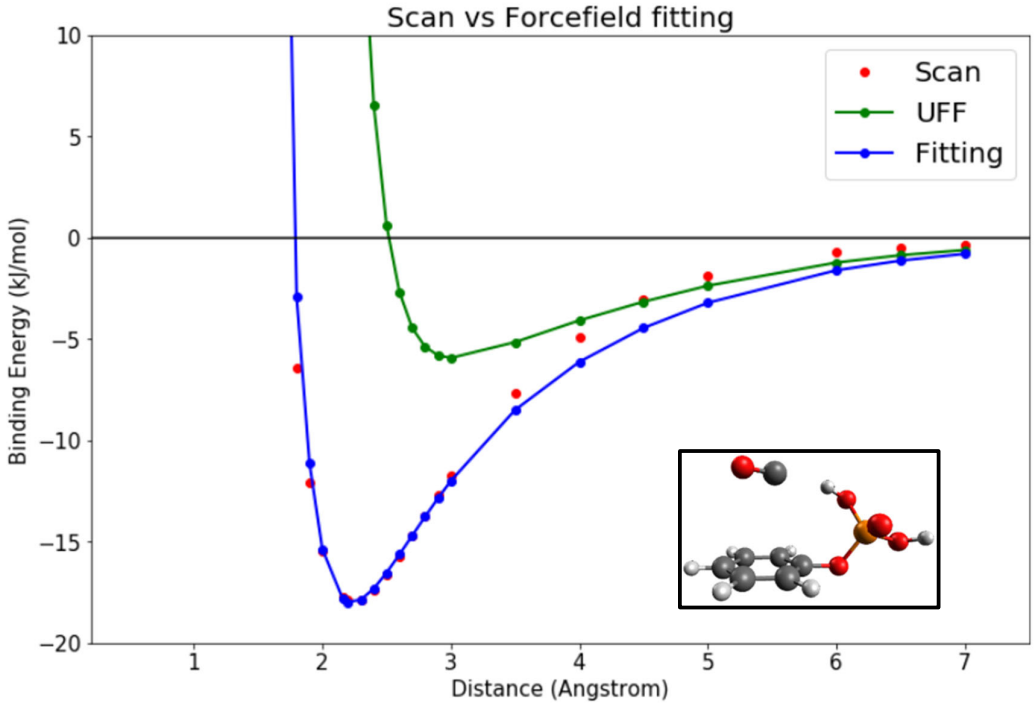

(b)

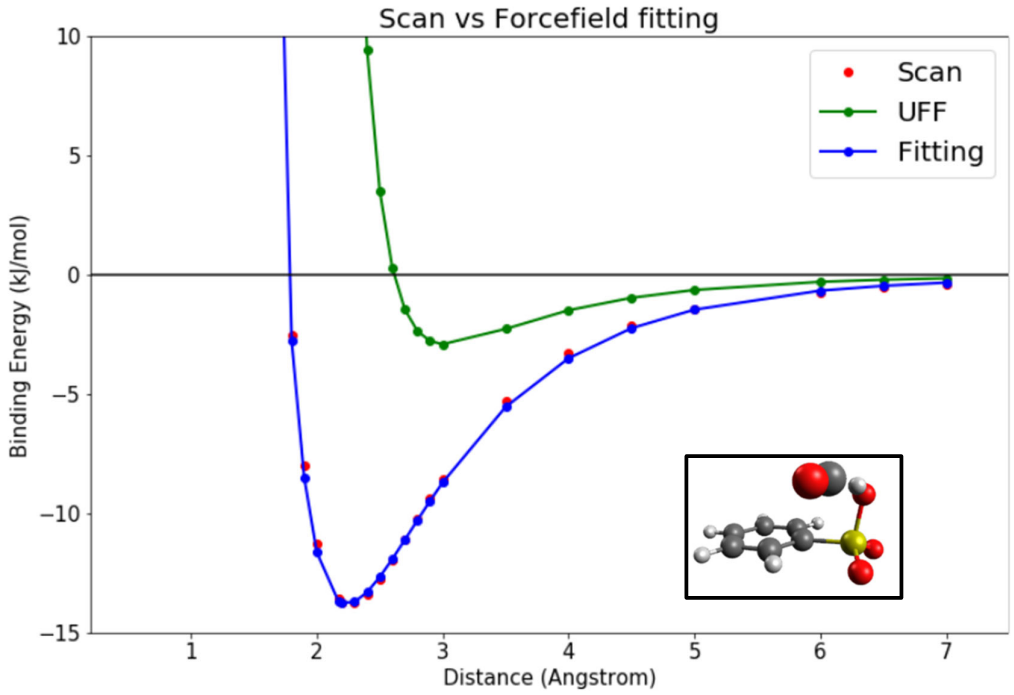

(c)

Figure S6: Fitting of the (ε, σ) parameters of the UFF potential on the QM data obtained from the ab-initio scan of CO over (a) C_6H_5-OSO_3H (b) C_6H_5-OPO_3H_2 (c) C_6H_5-SO_3H

The notable difference between UFF [27] and the ab-initio curve verifies the importance of the described fitting procedure and demonstrates the imminent danger of employing classical FFs without first checking their validity on the system under study.

GCMC results

Using the cluster approximation, we separated the ligand from its environment and terminated the hydroxyl groups with a Li atom to represent the effect of the charge density of the missing metal cluster. All 3 functionalized linker geometries were taken from geometry optimizations performed at the MP2/6-311++G** level of theory. For each structure, a cubic periodic box of size 30.09× 30.09 × 30.09 Å3 was used. The periodic box dimensions were large enough to ensure that no finite-size effects will affect the results. Initially, 50000 steps were conducted to let the system equilibrate. They were followed by 50000 production steps to calculate the average number of adsorbed molecules. This procedure was followed for each point of the isotherm uptake. The results from the GCMC simulations are depicted in Figure S7 where gravimetric (mmol/g) uptake and the volumetric (cm^3/cm^3) are shown for T=298K.

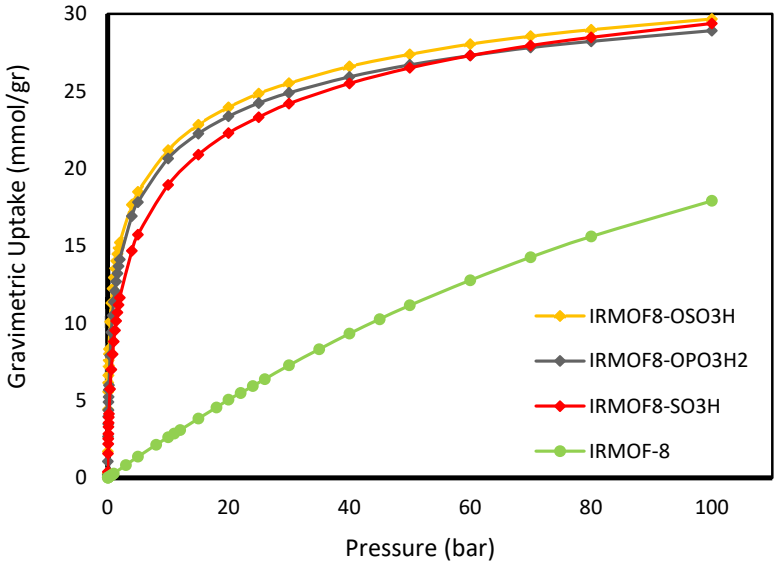

(a)

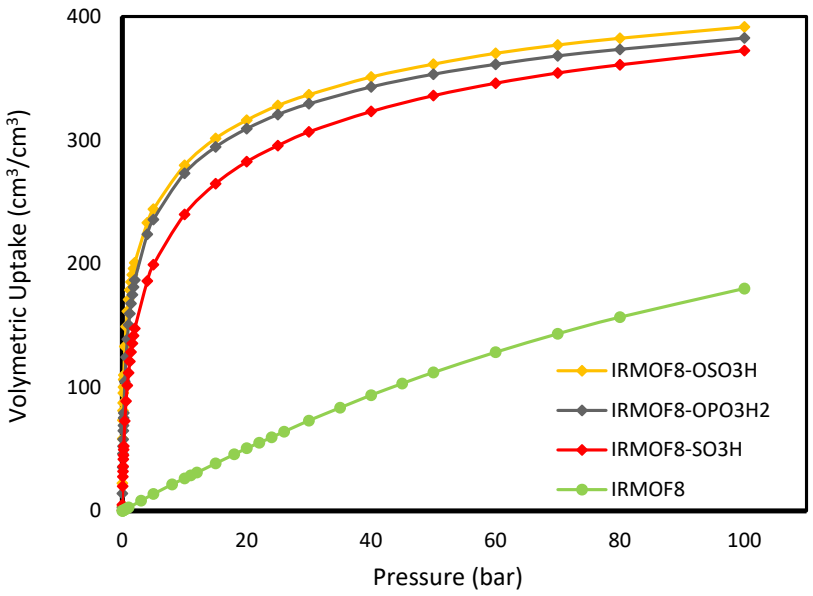

(b)

Figure S7: Gravimetric (a) and Volumetric (b) Carbon Monoxide uptake isotherms for IRMOF-8 and IRMOF-8-n (n: -OSO_3H, -OPO_3H_2, -SO_3H) at T=298K.

It can be clearly seen that the enhanced interaction of the functional groups with carbon monoxide, is reflected in the corresponding CO uptake of the modified IRMOF-8. The enhancement of the performance for the modified structures is more pronounced at the low loading limit i.e. the low-pressure range. This is expected since at this limit the adsorption is mainly defined by the interaction energy rather than other factors such as the pore volume and the surface area.

References

21 Neese, F. The ORCA program system. *WIREs Comput. Mol. Sci.* **2012**, *2*, 73–78. https://doi.org/10.1002/wcms.81

22 Neese, F. Software update: The ORCA program system, version 4.0. *WIREs Comput. Mol. Sci.* **2018**, *8*, e1327. https://doi.org/10.1002/wcms.1327

23 Boys, S.; Bernardi, F. The calculation of small molecular interactions by the differences of separate total energies. Some pro-cedures with reduced errors. Mol. Phys. 1970, 19, 553–566. https://doi.org/10.1080/00268977000101561

27 Rappe, A.; Casewit, C.; Colwell, K.; Goddard, W.; Skiff, W. UFF, a full periodic table force field for molecular mechanics and molecular dynamics simulations. J. Am. Chem. Soc. 1992, 114, 10024–10035. https://doi.org/10.1021/ja00051a040

30 Laaksonen, L. A graphics program for the analysis and display of molecular dynamics trajectories. J. Mol. Graph. 1992, 10, 33–34. https://doi.org/10.1016/0263-7855(92)80007-Z

31 Bergman, D.L.; Laaksonen, L.; Laaksonen, A. Visualization of solvation structures in liquid mixtures. J. Mol. Graph. Model 1997, 15, 301–206. https://doi.org/10.1016/S1093-3263(98)00003-5.

32 Berthelot D. Sur le mélange des gaz. Comptes Rendus Hebd Des Séances l'Académie Des Sci 1898;126:1703–855

33 Lorentz HA. Ueber die Anwendung des Satzes vom Virial in der kinetischen Theorie der Gase. Ann Phys 1881;248:127–36. https://doi.org/10.1002/andp.18812480110.